Journal of Inflammation Research

Dovepress
Taylor & Francis Group

Open Access Full Text Article

ORIGINAL RESEARCH

Integrated Single-Cell and Transcriptome Analysis with Experimental Validation Reveals PANoptosis-Related Gene Signatures in the Immune Microenvironment of Autoimmune Thyroiditis

Zhuo Zhao[1,*], Ziyu Liu[2,*], Qun Wang[3,4], Hao Gao[1], Nan Song[5], Xiao Yang[1,2]

[1]The Second Clinical College of Liaoning University of Traditional Chinese Medicine, Shenyang, Liaoning Province, People's Republic of China; [2]The Second Affiliated Hospital of Liaoning University of Traditional Chinese Medicine/Liaoning Institute of Traditional Chinese Medicine, Shenyang, Liaoning Province, People's Republic of China; [3]National and Local Joint Engineering Laboratory for Integrated Chinese and Western Medicine Prevention and Treatment Technology on Cardio-Brain Diseases, Liaoning University of Traditional Chinese Medicine, Shenyang, Liaoning Province, People's Republic of China; [4]Key Laboratory of Ministry of Education for TCM Viscera-State Theory and Applications, Liaoning University of Traditional Chinese Medicine, Shenyang, Liaoning Province, People's Republic of China; [5]College of Medical Laboratory, Liaoning University of Traditional Chinese Medicine, Shenyang, Liaoning Province, People's Republic of China

*These authors contributed equally to this work

Correspondence: Nan Song; Xiao Yang, Liaoning University of traditional Chinese Medicine, Shenyang, Liaoning Province, People's Republic of China, Tel +8613840575015, Email cpcool@126.com; yangxiaodyx@aliyun.com

Purpose: Autoimmune thyroiditis (AIT) is the most common organ-specific autoimmune disease, and its pathogenesis is closely related to the inflammatory microenvironment driven by immune cell penetration. The role of the newly proposed concept of PANoptosis in immune-related diseases is gradually being revealed. However, there is currently a lack of reports on PANoptosis in AIT. This study aims to clarify the relationship between PANoptosis gene, cell subgroup distribution, immune penetration, and AIT through a comprehensive analysis of scRNA-seq and bulk RNA-seq data combined with animal and clinical validation.

Patients and Methods: Initially, we integrated bulk RNA-seq and scRNA-seq data from AIT in public databases to identify immune cell subpopulations and the distribution and abundance of PANoptosis within them. Subsequently, we applied ssGSEA to assess the association between immune cell infiltration and inflammatory responses in AIT patients versus healthy individuals. Furthermore, we utilized the WGCNA tool to integrate PANoptosis genes with immune functions and screened for gene modules most significantly correlated with the immune-inflammatory effects of AIT. Finally, an animal model was established and clinical samples were collected for RT-qPCR, immunohistochemical staining,Enzyme-linked immunosorbent assay (ELISA) and ROC curve to predict the diagnostic value for further verification.

Results: Through bioinformatics analysis, we identified 14 functionally heterogeneous cell subpopulations and 5 differentially expressed PANoptosis-related genes (AIM2, ZBP1, NLRP6, MLKL, and FAS). Experimental validation revealed that these differentially expressed genes were significantly upregulated in autoimmune thyroiditis (AIT). Moreover, they might promote the infiltration of inflammatory lymphocytes and the secretion of inflammatory cytokines in thyroid tissue through the PANoptosis pathway, with AIM2 potentially playing a central role.

Conclusion: In summary, our study reveals the characteristics of the immune microenvironment of AIT and highlights the clinical potential of PANoptosis-Related genes (AIM2, ZBP1, NLRP6, MLKL, and FAS) as diagnostic biomarkers.

Keywords: autoimmune thyroiditis, PANoptosis, single-cell RNA sequencing, bulk RNA-sequencing, immune microenvironment, biomarkers

Introduction

Autoimmune thyroiditis (AIT) represents not only the most prevalent thyroid autoimmune disorder but also one of the most common autoimmune diseases, with Hashimoto's thyroiditis (HT) being its primary type.[1] In recent decades, the incidence and prevalence of AIT have witnessed a sharp increase, attributed to societal developments and changes in

Received: 21 March 2025
Accepted: 11 July 2025
Published: 3 September 2025

lifestyle habits, reaching a global prevalence of approximately 7.5%.[2] The pathogenesis of AIT is intricate, primarily attributed to the disruption of immune tolerance induced by environmental and genetic factors, leading to anti-thyroid autoimmune responses.[3] This manifests as elevated levels of thyroid-specific autoantibodies accompanied by diffuse lymphocytic infiltration in thyroid tissues. It has been reported that cytokines secreted by lymphocytes serve as major regulators of thyroid immune injury, stimulating thyroid cells to autonomously release proinflammatory mediators, thereby amplifying and sustaining autoimmune responses.[4] Despite compelling clinical and epidemiological evidence suggesting an interplay between immune cell populations and the thyroid inflammatory microenvironment, the underlying common mechanisms and crucial molecular signatures governed by genetic regulation remain largely unknown.

PANoptosis is a new concept, which was put forward by American scholar Malireddi in 2019.[5] It represents a novel form of innate immune inflammatory programmed cell death (PCD). This process is primarily regulated by the PANoptosome complexConcurrently, it triggers the secretion of cytokines, instigating an intracellular signaling cascade that stimulates the production of pro-inflammatory cytokines and subsequently elicits an inflammatory response, ultimately leading to the occurrence of PANoptosis.[6,7] PANoptosis is a phenomenon characterized by the interplay and overlap among pyroptosis, apoptosis, and necroptosis (P, pyroptosis; A, apoptosis; N, necroptosis). Research has demonstrated that PANoptosis exhibits significant pathophysiological correlations with inflammation and autoimmunity.[8] Emerging evidence suggests that PANoptosis can contribute to autoinflammation, neuroinflammation, and metabolic inflammation, exerting widespread effects throughout the body and potentially serving as a pivotal regulator in autoimmune diseases.[9] Given the existing gaps in understanding the potential regulatory mechanisms of PANoptosis in AIT, our previous findings revealed marked activation of the NLRP3 inflammasome, which mediates pyroptosis, in the thyroid tissue of AIT mice.[10] Mo K et al[11] discovered that targeting hnRNPC can inhibit apoptosis and necroptosis of thyroid follicular epithelial cells through m6A modification of ATF4. It is evident that apoptosis, pyroptosis, and necroptosis are key mechanisms regulating the progression of AIT. However, a single type of PCD appears insufficient to fully explain the disease development process. Therefore, it is reasonable to speculate that PANoptosis, which integrates the characteristics of these PCDs, may play a significant role in the progression of AIT and warrants further exploration.

Autoimmune diseases are mostly attributed to the massive release of immune cytokines, resulting in uncontrollable inflammatory responses across various bodily systems. Identifying and determining the immune cell populations that play a dominant role in the onset and progression of AIT, namely the key immune cell types, is crucial for enhancing our understanding of the pathogenesis of AIT. Single-cell RNA sequencing (scRNA-seq), which delineates the global gene expression profile of individual cells, has emerged as a revolutionary tool for unveiling the heterogeneity of complex tissues, elucidating disease pathogenesis, and facilitating the development of innovative therapeutics.[12] This technology has been recognized as the "Method of the Year" by the prestigious journal Nature.[13] However, studies utilizing scRNA-seq in AIT, particularly those delving into the associations between pan-apoptotic genes, immune infiltration, and HT, remain scarce.

In this study, we integrated bulk RNA-seq and scRNA-seq data of AIT from public databases. Utilizing tools such as Weighted Gene Co-expression Network Analysis (WGCNA), we identified aberrantly expressed immune cells at both the global and single-cell levels. Furthermore, we elucidated the interplay between PANoptosis, cellular subpopulation distribution, and immune cell infiltration, along with the identification of core genes. A gene co-expression network was constructed, followed by experimental validation. Collectively, our findings revealed the pivotal regulatory role of PANoptosis in the progression of AIT and identified the core genes involved. These insights have not only enhanced our understanding of the underlying mechanisms of AIT and identified potential novel biomarkers, but also laid the foundation for future in-depth exploration of the regulatory role of PANoptosis in AIT and the immunoregulatory network.

Materials and Methods

Gene Data Source and Preprocessing

The scRNA sequencing dataset HRA001684 was retrieved from the official NGDC website [NGDC–GSA for Human (cncb.ac.cn)]. The HRA001684 dataset comprises scRNA sequencing data from 5 samples and bulk-RNA seq data from 66 samples. The scRNA sequencing dataset HRA001684, which encompasses peripheral blood mononuclear cells

(PBMCs) and thyroid tissue samples derived from patients with Hashimoto's thyroiditis (HT), was subjected to analysis. The sequencing data in question was acquired through the utilization of the 10x Genomics scRNA-seq platform. The bulk data consist of thyroid tissue samples from 50 non-HT individuals and 16 HT patients. Primary thyrocytes were isolated via a modified Morgan et al method. Normal thyroid tissues from thyroidectomy patients were minced, washed, and digested with collagenase II, dispase, and FBS at 37 °C. After filtration and centrifugation, cells were treated with lysis buffer to remove erythrocytes, then filtered again. Dead cells were removed, yielding over 90% viable cells. PBMCs were isolated from 5 mL EDTA-K2 anticoagulant blood via density gradient separation using lymphoprep, collected pre-operation for scRNA-seq in 10x Genomics scRNA-seq platform. The relevant information is shown in Table 1. Initially, gene IDs in the bulk data were converted, and duplicate gene IDs were removed. After preprocessing, 35,152 genes remained. Subsequently, quality control was performed, including trimming adapters, sequence alignment, and expression quantification. Finally, count values were utilized for downstream analyses. The PANoptosis genes were sourced from an article published in Nature magazine.[14]

Processing of Single-Cell RNA (scRNA) Sequencing Data

Firstly, we processed the single-cell data using Seurat to filter cellular subpopulations. The criteria for cell filtering were set as having 200–4000 unique molecular identifiers (UMIs) and a mitochondrial content of less than 10%. After filtering, 107,975 cells remained for subsequent analysis. Principal Component Analysis (PCA) was performed using the ScaleData function to reduce and dimensionally downscale all genes. Subsequently, the FindNeighbors and FindClusters functions (with a resolution setting of 0.1) were utilized to cluster individual cells, determine cellular subgroups, and annotate each subgroup accordingly. Marker genes were used to label each cell cluster. Finally, the PANoptosis gene was integrated with the cellular subpopulations, and the distribution and abundance of the PANoptosis gene[14] within the AIT cellular subgroups were analyzed. DEGs between the HT and non-HT groups were selected in the HRA001684 dataset by using the DEseq2 package (v 1.36.0) with adjusted P value < 0.05 and |log2FC| > 1.

Analysis of Immune Infiltration and Immune Scores

It has been demonstrated that single-sample gene set enrichment analysis (ssGSEA) can be used to quantify the correlation between immune cells and their functions.[15] The ssGSEA was performed to find the enriched regulatory pathways and biological functions of biomarkers with P value < 0.05 and |NES| > 1. Therefore, based on the integrated biological data, we employed ssGSEA to evaluate the correlation between single-sample genes of immune cells and their functions, and visualized the results as a heatmap. Finally, we utilized R packages to visualize the correlation between immune cells and inflammation. Spearman correlation analysis was applied for statistical purposes, and significance was determined at a threshold of $P < 0.05$. Subsequently, the ggplot2 and reshape2 packages in R were used for data transformation and visualization to assess the differences in immune scores between non-HT individuals and HT patients.

Key Module Genes Were Screened by Weighted Gene Correlation Network Analysis

Utilizing the "WGCNA" package in R software, we studied the associations between genes and phenotypes by constructing a gene co-expression network.[16] Initially, samples were clustered to eliminate outliers and ensure the accuracy of the analysis. Next, to approximate a scale-free topology for the network, we selected the optimal soft threshold. When the soft threshold was set to 16, the interactions among genes conformed to the scale-free distribution to the greatest extent, with an R^2 value of 0.9 and the average connectivity approaching zero. Subsequently, a clustering dendrogram was obtained by calculating adjacency and similarity measures. Finally, we computed the dissimilarity of module eigengenes, selected a cut-off line for the dendrogram to

Table 1 Database Information

Sequencing Type	Non-HT Individuals	HT Patients	Species	Sample Type
Bulk	50	16	non-HT patients	thyroid
scRNA	0	5	HT patients	PBMC, thyroid

https://doi.org/10.2147/JIR.S525270

define modules, and merged several modules. WGCNA was employed to identify significant modules in the disease context and to create a visual representation of the characteristic gene network.

Mice and Groups

The NOD.H-2^{h4} mice, an optimal model for AIT, were chosen as the research subjects. The mice (Strain: No. 004447, age: 8–10 weeks, weight: 20 ± 2 g) were obtained through Jackson Laboratory (Bar Harbor, ME, USA). They were housed in the Experimental Animal Center Laboratory of Liaoning University of Traditional Chinese Medicine under pathogen-free (SPF) conditions, with a temperature of 22°C ± 1°C, humidity at 50% ± 5%, and natural light exposure.

Sixteen 8-week-old mice were randomly allocated into the following groups: control group (Control), model group (Model), each comprising 8 mice. The control group was provided with sterile distilled water, while the AIT group received an aqueous solution containing 0.05% NaI for ad libitum drinking for a duration of 8 weeks. At the end of the 8-week period, the mice were euthanized, and peripheral blood and thyroid samples were collected for subsequent experiments.

Study Participants

Peripheral blood samples from 40 AIT patients and age/sex-matched healthy controls were collected, processed, and analyzed. All participants provided written informed consent under protocols approved by the Institutional Review Board. Subjects were categorized into AIT and healthy control (HC) groups for comparative analysis.

Enzyme-Linked Immunosorbent Assay (ELISA)

The levels of TGAb and TPOAb were assessed in serum using enzyme-linked immunosorbent assay (ELISA) kits (Shanghai Enzyme-Linked Biotechnology Co., Ltd., Shanghai, China) according to the manufacturer's instructions.

Hematoxylin and Eosin (H&E) Staining

Thyroid tissues from mice in each group were fixed, dehydrated, and embedded in a gradient, then sectioned into 5 μm slices. Following dewaxing, rehydration, and hematoxylin staining for 5 minutes, differentiation was performed using color separation solution. Sections were then dehydrated, stained with eosin, treated for transparency, and sealed. Pathological changes were observed in random visual fields under a high-power microscope (Beyotime, Shanghai, China). To assess thyroid inflammation, scores were assigned based on the extent of lymphocyte infiltration:0 = normal; 1 = no infiltration; 2 = 10–30% of total area; 3 = 30–50% of total area; 4 = >50% of total area.

Quantitative Real-Time PCR (qRT-PCR)

Following Trizol reagent instructions (CWBIO, Beijing, China), total RNA was extracted from thyroid tissue. Genomic DNA was removed using a reverse transcription kit (CWBIO, Beijing, China). GAPDHserved as the internal reference mRNA. Quantitative analysis was performed using Magic SYBR Mixture (CWBIO, Beijing, China), and the $2^{-\Delta\Delta CT}$ method was used to analyze mRNA levels of target genes. Primer sequences are listed in Table 2. Relative mRNA expression levels were compared to the normalized Sham group. Primer sequences were listed in Table 2.

Immunohistochemistry

Thyroid tissue sections underwent antigen retrieval in citrate buffer, endogenous peroxidase was quenched with 3% H_2O_2, and sections were incubated. Primary antibody AIM2, ZBP1,NLRP6, MLKL,FAS (1:200, Proteintech Group, Inc, Hubei, China) was added and incubated overnight. After PBS rinse, secondary HRP-conjugated antibodies were applied, followed by DAB staining, hematoxylin counterstaining, and sealing. Images were captured using an optical microscope (Olympus Corporation, Japan) and analyzed with Image J.

Table 2 Primer Sequence of the Gene

Genes	Primer Sequences	Product Length/bp	Species
AIM2	F: 5′-GGGTGGCGTCAGGAAGTTTT-3′	183	Mouse
	R: 5′-CTTCCTCCGTGATGTGGTCC-3′		
	F: 5′-CAGGAGGAGAAGGAGAAAGTTGAT-3′	137	human
	R: 5′-ACTTTTGGTGCAGCACGTTG-3′		
ZBP1	F: 5′-GACTTGAGCACAGGAGACAAT −3′	113	Mouse
	R: 5′- GTTTTCTTGGGCACTTGGCAT-3′		
	F: 5′-CGGGCAGAGAAGGCCAC-3′	119	human
	R: 5′-TTGGTTGAGCTCCCTCTTGG-3′		
MLKL	F: 5′-TCTGGCAGAGAACGAATCTTG −3′	130	Mouse
	R: 5′-TTTGCTCCCAGCAATAAGTTGA-3′		
	F: 5′-GATCAGCAGGATGCAGACGA-3′	141	human
	R: 5′-GGACGATTCCAAAGACTGCC-3′		
NLRP6	F: 5′-TTCTCTCCGTGTCAGCGTTC −3′	87	Mouse
	R: 5′-CAGAGCGAGCATTCCTCTCC-3′		
	F: 5′-CAAAACAACTGCCAGCCTCC-3′	91	human
	R: 5′-CAGTGGGACAGCGTGAGG-3′		
FAS	F: 5′-GTCCTGCCTCTGGTGCTTG-3′	148	Mouse
	R: 5′-AGCAAAATGGGCCTCCTTGAC-3′		
	F: 5′-GACCCTCCTACCTCTGGTTCT-3′	184	human
	R: 5′-ACCTGGAGGACAGGGCTTAT-3′		
GAPDH	F: 5′-CAGGAGAGTGTTTCCTCGTCC-3′	188	Mouse
	R: 5′-TGCCGTGAGTGGAGTCATAC-3′		
	F: 5′-ATTCCATGGCACCGTCAAG-3′	84	human
	R: 5′-GAGGGATCTCGCTCCTGG-3′		

ROC Analysis

ROC curves were generated using R (v4.2.1) with the pROC package (v1.18.0) for AUC calculation and outcome-order correction. Visualization was implemented via ggplot2 (v3.4.4). Diagnostic performance was quantified through bootstrapped 95% confidence intervals (1,000 iterations).

Statistical Analysis

Statistical analyses were conducted using R (Version 4.2.2) and GraphPad Prism (Version 9.5.0). For comparisons between two groups, independent sample *t*-tests were applied for normally distributed continuous variables, whereas Mann–Whitney *U*-tests were used for non-normally distributed continuous variables. The flow chart of this research was shown in Figure 1.

Results

Single-Cell RNA Sequencing Analysis and Unbiased Clustering of HT Patients

Our study utilized a scRNA sequencing dataset (HRA001684) obtained from NGDC. After quality control, cell filtering, and standard data processing, we obtained 107,975 cells from thyroid and peripheral blood tissues of 5 HT patients for subsequent analysis (Figure 2A and B). Subsequently, UMAP was employed for dimensionality reduction, clustering, and visualization of the dataset (Figure 2C). The scRNA sequencing data were divided into 15 major cell clusters using the "FindNeighbors" and "FindCluster" functions, and represented through UMAP analysis (Figure 2D). Based on the canonical patterns of marker genes, these clusters were further classified into 14 cell subtypes: B cell, CD8+T cell, endothelial cell, fibroblast, macrophage, myeloid cell, neutrophil, NK cell, plasma cell, platelet, proliferating cell, smooth muscle cell, T cell, and thyroid cell (Figure 2E). To define the identity of each cell cluster, we manually categorized the

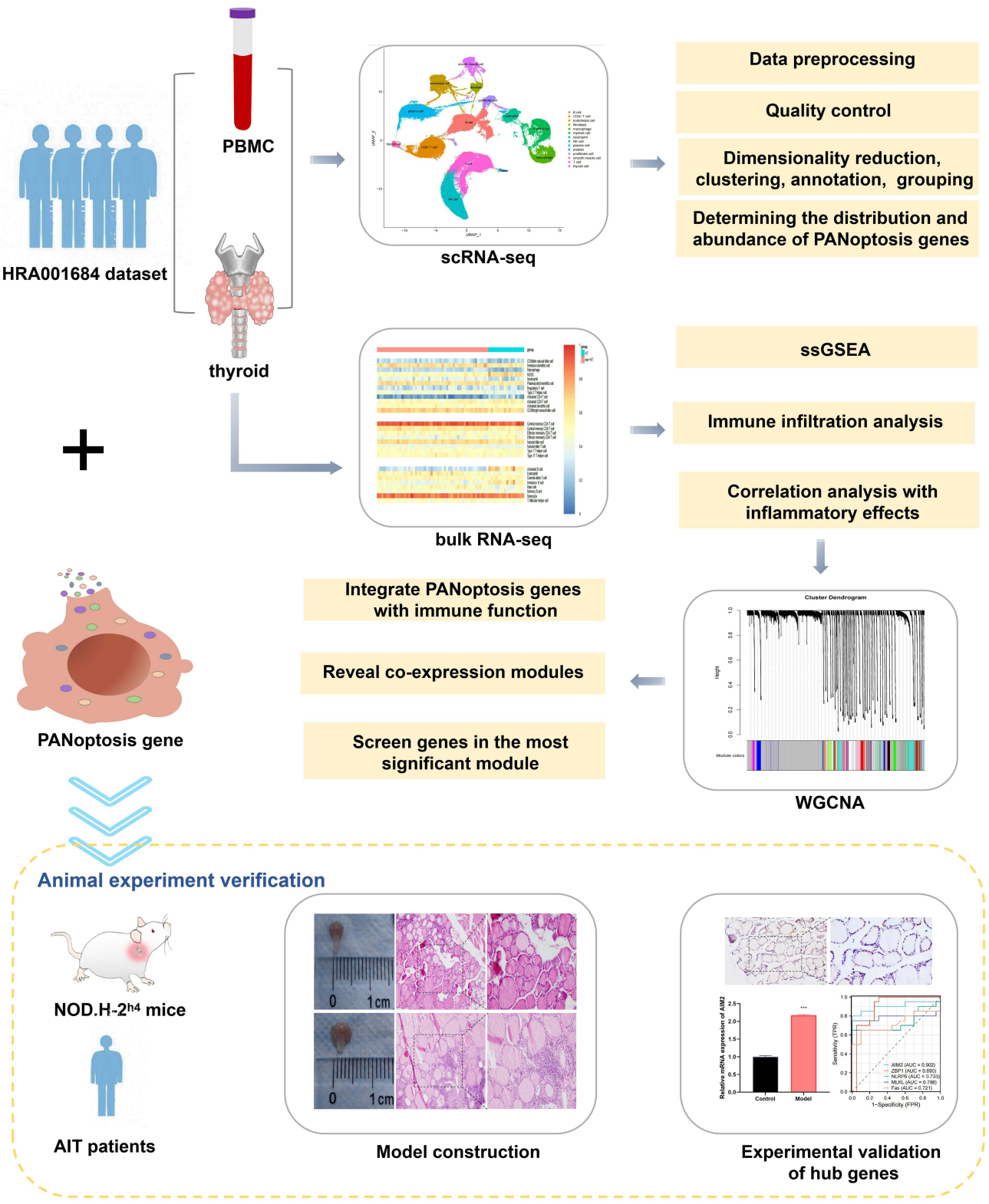

Figure 1 The flow chart of this research.

clusters into known cell type populations based on the differential expression of both known and novel marker genes. The typical marker genes specifically expressed in each cell cluster further validated our cell type annotations (Figure 2F). The results are presented in a marker gene bubble plot, where the x-axis represents marker genes, the

y-axis represents cell types, the size of the dots represents the percentage of cells expressing each gene, and the color of the dots represents the expression level. This suggests that they may be key cell populations involved in the progression of AIT, warranting further investigation.

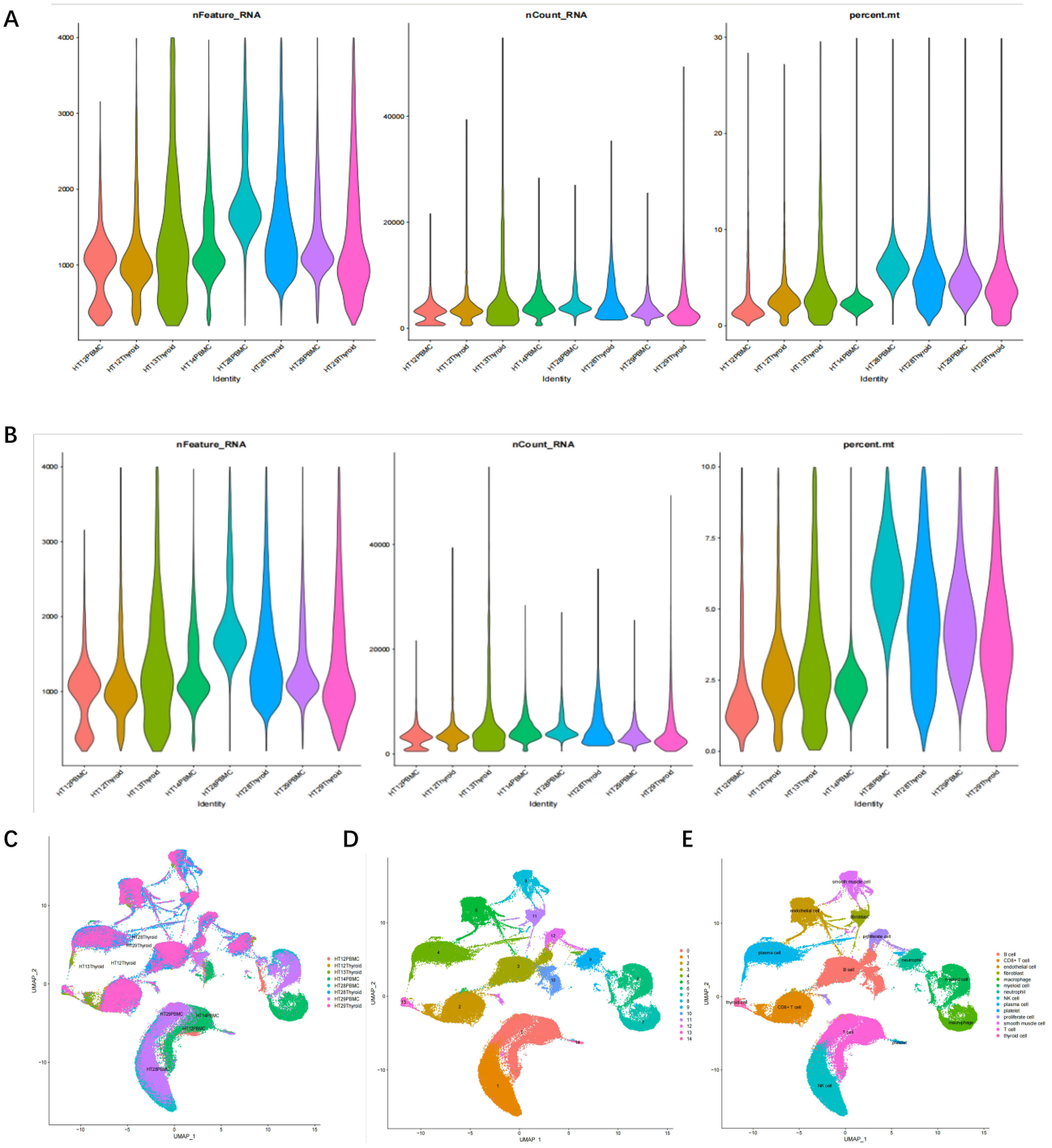

Figure 2 Continued.

https://doi.org/10.2147/JIR.S525270

Figure 2 Single-cell RNA sequencing analysis and unbiased clustering of HT patients:UMAP PLOT. (**A**) Violin plot before cell filtering. (**B**) Violin plot after cell filtering. (**C**) UMAP plot of samples from 8 HT patients after quality control, colored by data source (pbmc or thyroid) and cluster identity. (**D**) UMAP plot annotated with Seurat clusters after clustering of 107,975 cells, colored by cluster identity (0–15). (**E**) UMAP plot annotated by cell type after clustering, colored by subpopulation identity. (**F**) Dot plot of marker genes matching cell type annotations.

scRNA-Seq Reveals the Distribution Characteristics of PANoptosis Genes Across Various Cell Clusters

PANoptosis, a newly discovered form of cell death in recent years, despite numerous reports highlighting its association with the onset and progression of autoimmune-related diseases, lacks corresponding reports in the context of AIT (Autoimmune Thyroid Disease). To explore the role of panoptosis in the progression of AIT, we analyzed the distribution and abundance of the PANoptosis gene set across various cellular subpopulations (Figure 3A). Intriguingly, we found that panoptosis-related genes are expressed in multiple cell types, with the panoptosis gene AIM2 being most prominently expressed in proliferating cells (cells with potential differentiation capacity) (Figure 3B), suggesting that AIM2, as an important innate immune sensor, may regulate the progression of AIT through mediated PANoptosis.

Evaluation and Correlation Analysis of Immune Cell Infiltration

ssGSEA is an immune analysis method that scores individual samples based on immune-related gene sets to assess the expression levels of various immune infiltration-related cells in the samples. Therefore, we performed an immune infiltration analysis on thyroid tissues from 50 non-HT individuals and 16 HT patients in the Bulk dataset. The results, presented in a heatmap of immune cells for the two patient groups, revealed three distinct layers. The first layer consists of immune cells that inhibit inflammation, namely: CD56dim natural killer cell, Immature dendritic cell, Macrophage, MDSC, Neutrophil, Plasmacytoid dendritic cell, Regulatory T cell, Type 2 T helper cell, Activated $CD4^{+}$T cell, Activated $CD8^{+}$T cell, Activated dendritic cell, and CD56bright natural killer cell. The second layer comprises pro-inflammatory immune cells, including: Central memory $CD4^{+}$T cell, Central memory $CD8^{+}$T cell, Effector memory $CD4^{+}$T cell, Effector memory $CD8^{+}$T cell, Natural killer cell, Natural killer T cell, Type 1 T helper cell, and Type 17 T helper cell. The third layer includes other immune cells, such as Activated B cell, Eosinophil, Gamma delta T cell, Immature B cell, Mast cell, Memory B cell, Monocyte, and T follicular helper cell (Figure 4A). We further applied ssGSEA to evaluate the correlation of inflammatory effects between the HT group and the control group. The results showed that, The horizontal axis represents the anti-inflammatory effect, and the vertical axis represents the pro-inflammatory effect. Upon further comparison of the pro-inflammatory effects between HT patients and non-HT patients, it was found that the pro-

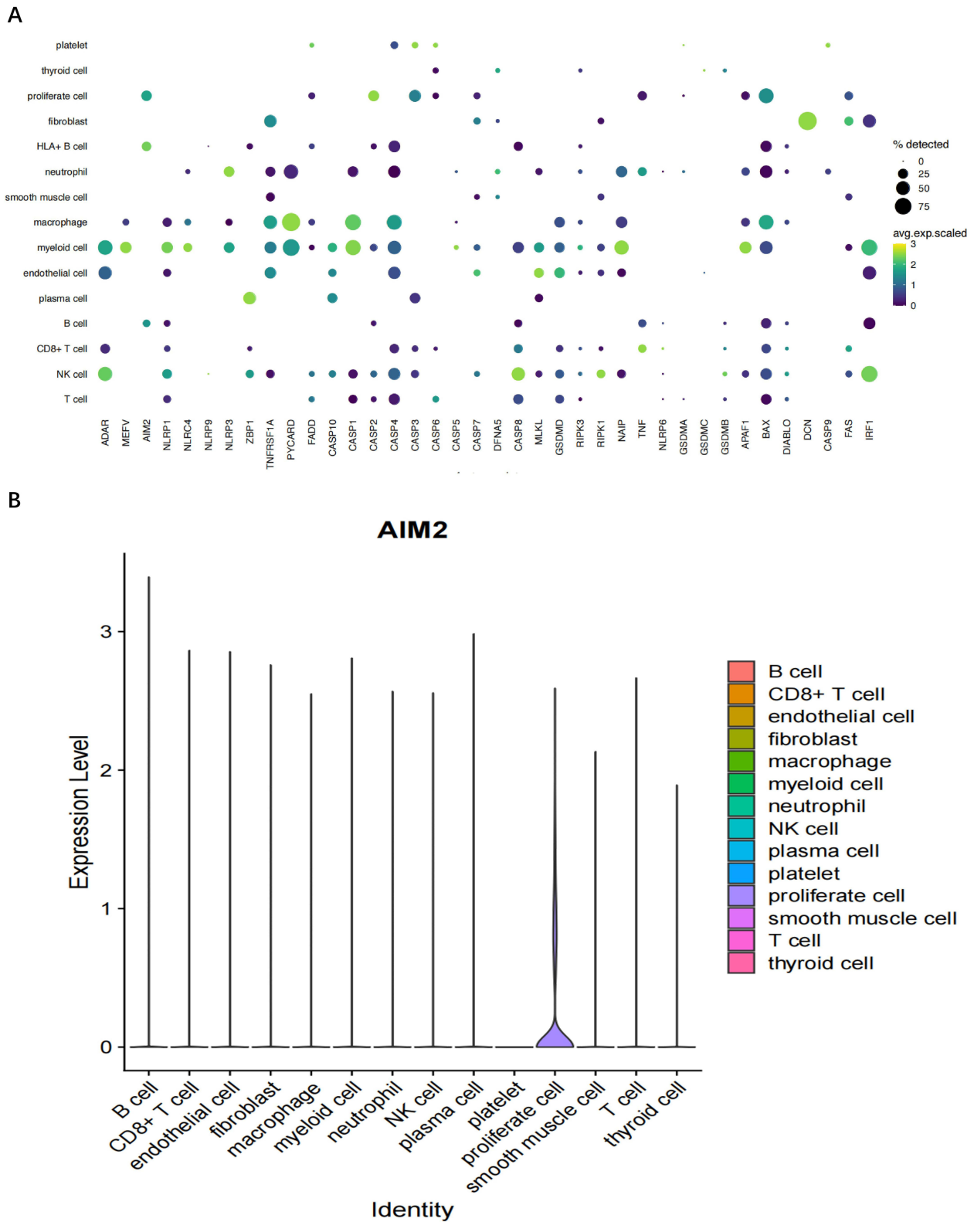

Figure 3 scRNA-seq reveals the distribution characteristics of PANoptosis genes across various cell clusters. (**A**) Bubble plot displaying the expression levels of pan-apoptotic genes with matched cell type annotations; (**B**) Violin plot showing the expression levels of the AIM2 gene across various cell type clusters. The y axis shows the normalized read count.

https://doi.org/10.2147/JIR.S525270

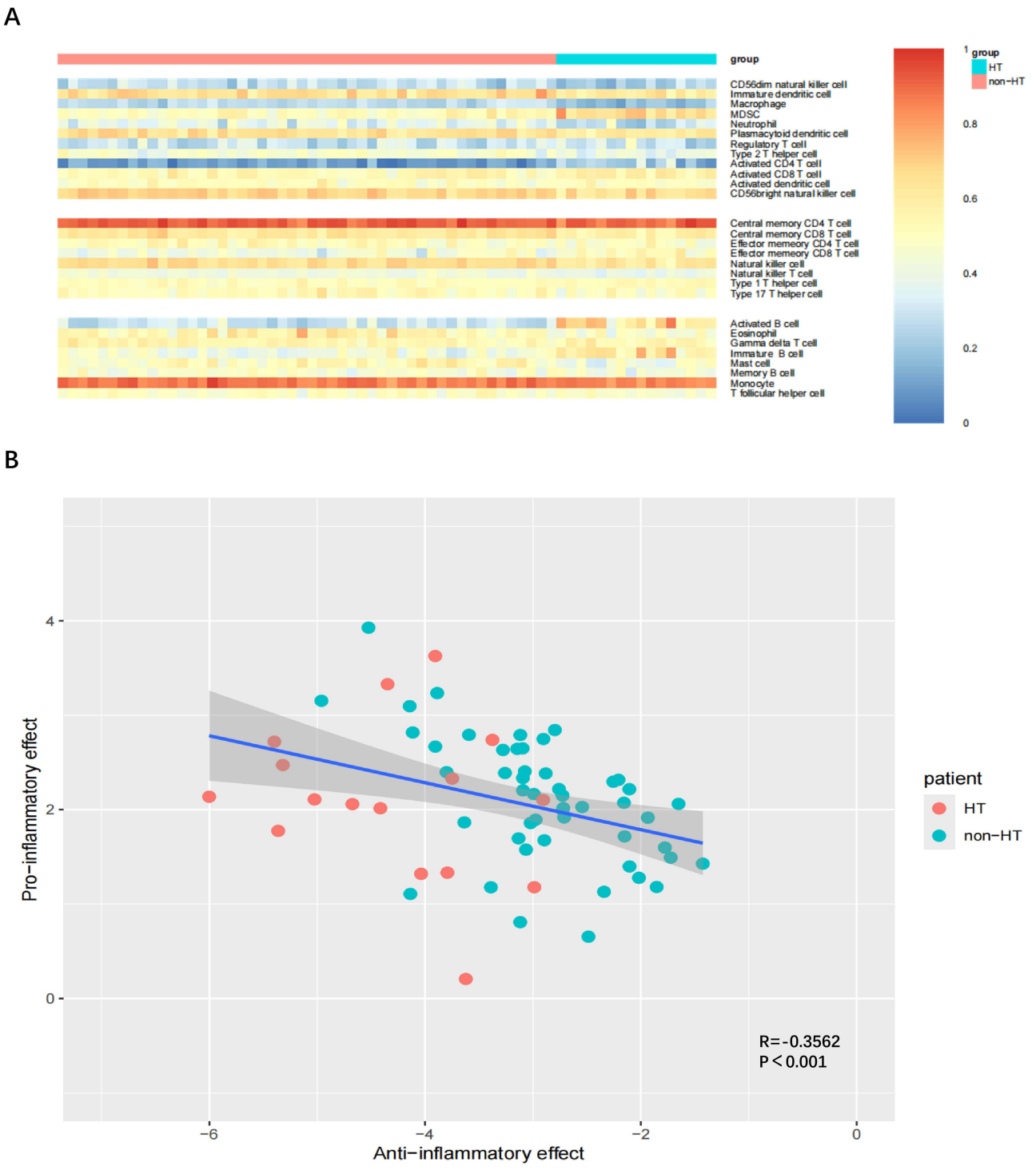

Figure 4 Evaluation and correlation analysis of immune cell infiltration. (**A**) Heatmap of immune cells in two patient groups. The heatmap displays the cell types and inflammatory effects of immune cells in the two patient groups. Red represents high expression levels, while blue represents low expression levels. (**B**) Correlation analysis evaluating immune cells and inflammatory effects in the two patient groups, with HT individuals represented in red and non-HT individuals in blue.

inflammatory effect values of HT patients were generally higher than those of non-HT patients. HT patients exhibited a stronger pro-inflammatory effect (r =–0.3562). (Figure 4B), identifying pro-inflammatory and anti-inflammatory subsets of immune cells that may be involved in the regulation of immune inflammation in HT patients. Detailed results of the immune scoring are provided in Supplementary Table S1.

WGCNA Analysis and Identification of Candidate Hub Genes

The construction of the WGCNA network and the identification of immune-related modules and hub genes were aimed at gaining deeper insights into the roles of different immune types in HT and inflammatory responses.[16] Firstly, we determined the optimal soft threshold through calculations, and the results showed stable average connectivity, indicating good network connectivity (parameters: soft threshold = 16) (Figure 5A and B). Subsequently, a weighted gene co-expression network was constructed, and genes with highly correlated expression were classified into the same color module using WGCNA analysis (totaling 67 co-expression modules) (Figure 5C). Correlation analysis was then performed between these modules and immune functions, and the correlations of different modules with the Anti-immune score, Pro-immune score, and HT were calculated (Figure 5D). We found that Module 5 (CD5.green) exhibited the strongest correlation with HT and pro-inflammatory responses. Intriguingly, we also identified PANoptosis-related genes within Module 5, including AIM2, ZBP1, MLKL, NLRP6, and Fas. Among these, the AIM2 gene emerged as a potential core hub gene (kme = 0.55) in the PANoptosis pathway.

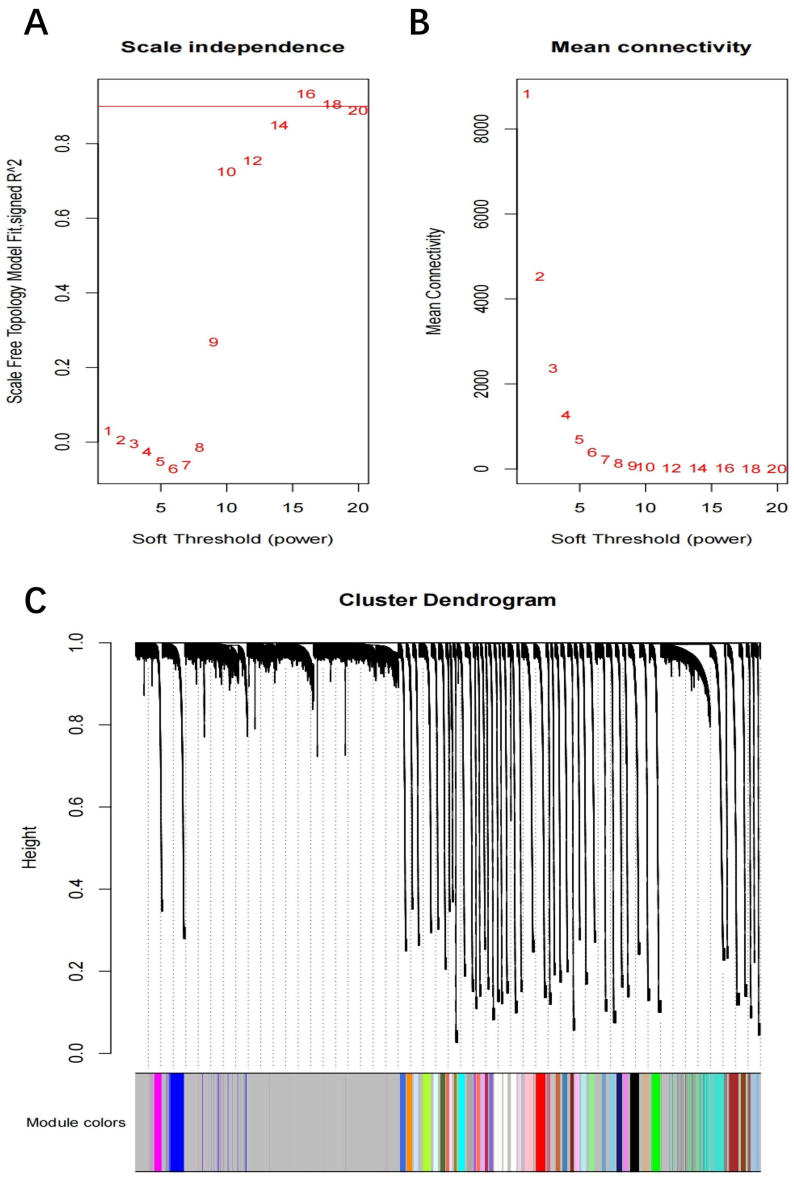

Figure 5 Continued.

https://doi.org/10.2147/JIR.S525270

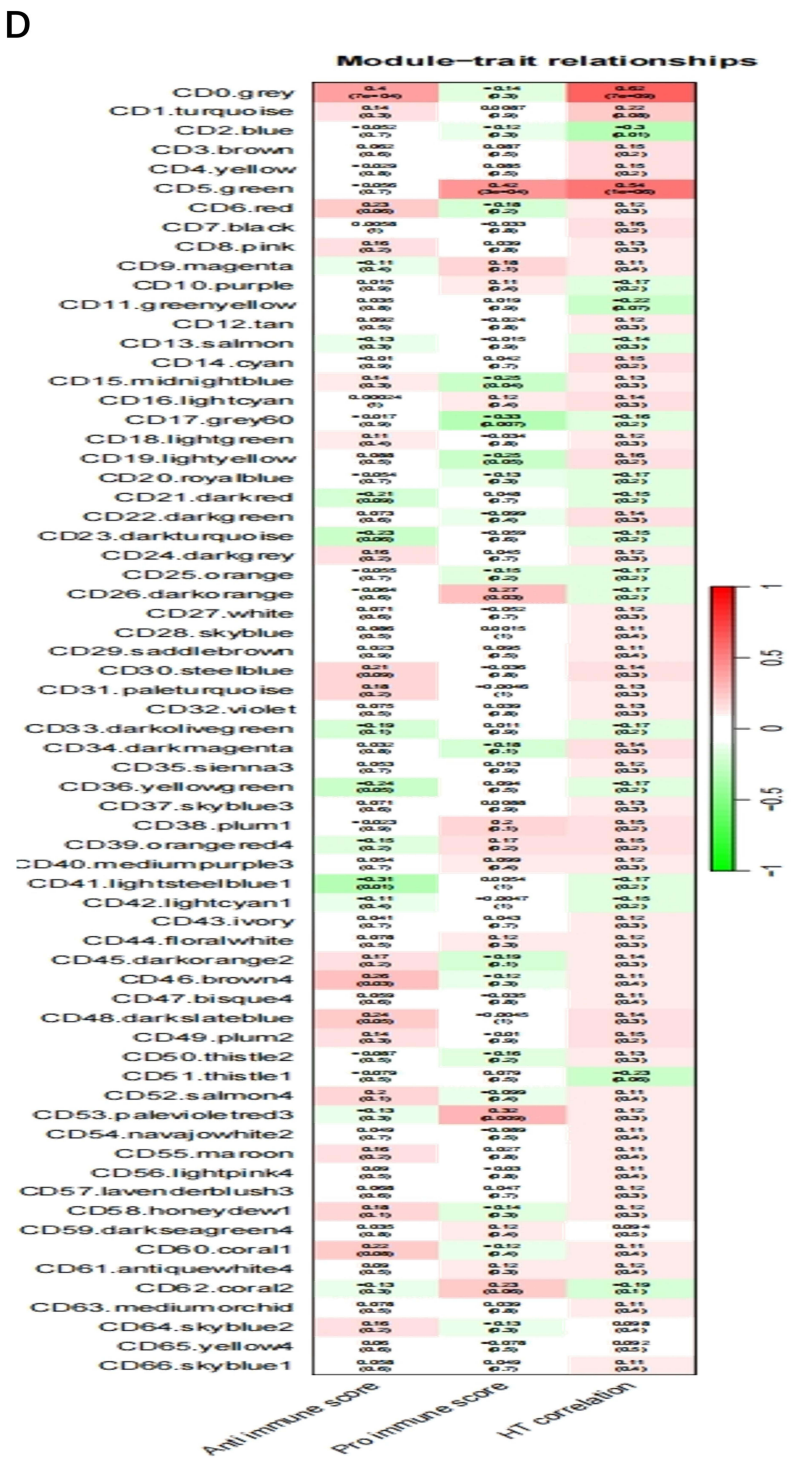

Figure 5 WGCNA Analysis and Identification of Candidate Hub Genes. (**A**) Soft thresholding power for WGCNA. (**B**) Mean connectivity in WGCNA. (**C**) Gene clustering dendrogram. (**D**) Correlation of WGCNA modules with Anti-immune score, Pro-immune score, and HT.

Construction of an AIT Animal Model

The NOD.H-2^{h4} mice has emerged as a prototype model for human AIT. Therefore, we initially selected 16 NOD.H-2^{h4} mice imported from The Jackson Laboratory in the USA. These mice were allowed free access to 0.05% sodium iodide water for 8 weeks (Figure 6A) to establish the model, followed by model validation. We observed that the thyroid

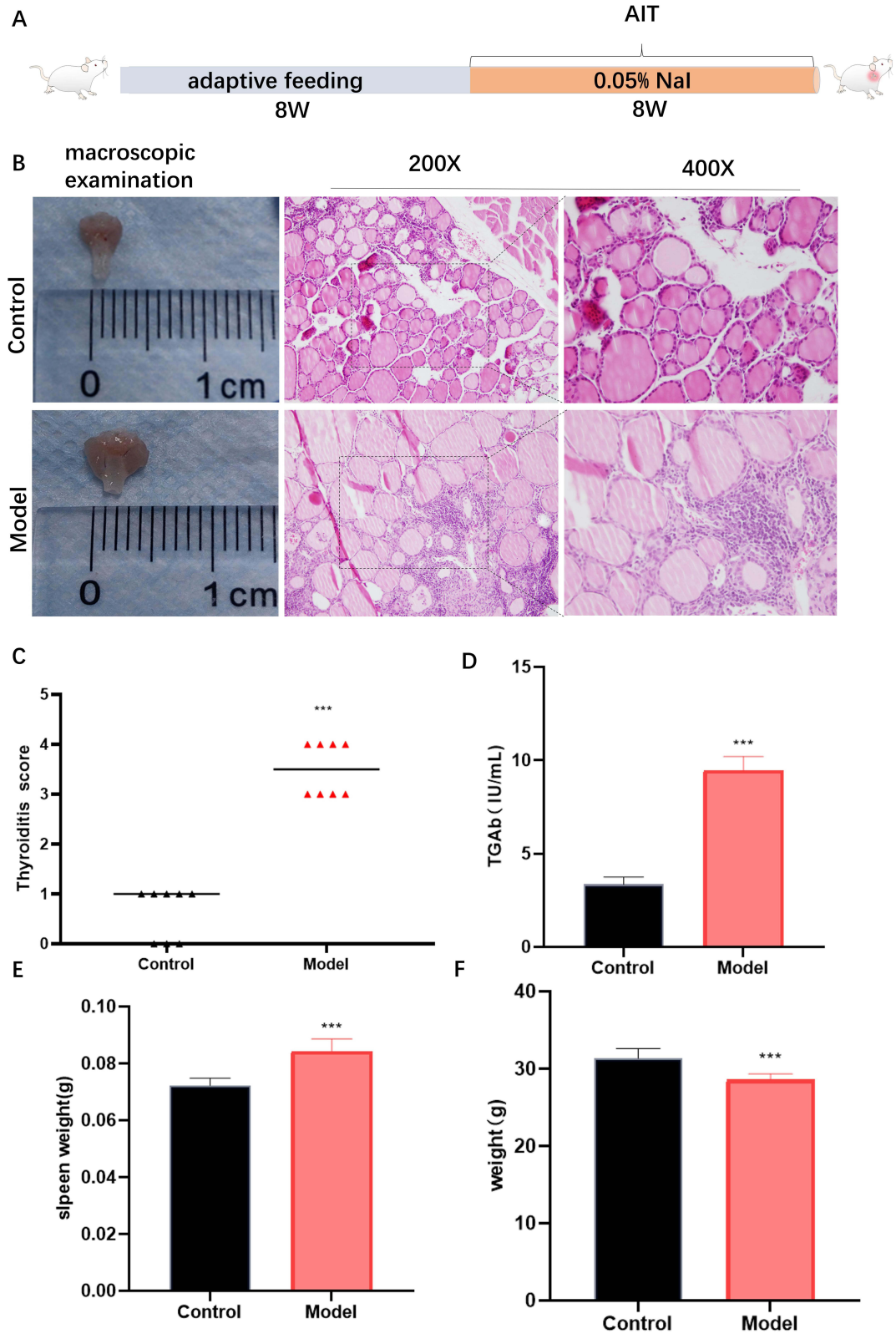

Figure 6 Construction of an animal model Establish an animal model:Schematic diagram of NOD.H-2^{h4} mice modeling. (**A**) Schematic diagram of model construction. (**B**) Representative images of H&E staining of thyroid tissue (original magnification, 200×,400×) (**C**) inflammatory infiltration score of thyroid tissue (n=8) (**D**) The content of TgAb in serum (n=8). (**E**) Data statistics of the spleen (n=8). (**F**) Mice body weight.***$P < 0.001$ vs. Control group.

https://doi.org/10.2147/JIR.S525270

follicular epithelial cells in the Control group were structurally intact, regularly arranged, uniform in size, and abundant in colloid, with occasional lymphocytes present. In contrast, the thyroid tissue of the model group exhibited marked enlargement upon gross examination. HE staining revealed significant disruption of the thyroid follicular structure, with follicles varying in size, disordered arrangement, reduced mesenchyme, and diffuse lymphocyte infiltration within the follicular lumina and interstitium, indicating severe inflammation (Figure 6B). The inflammation score was significantly elevated (Figure 6C, $P < 0.001$), and the TGAb levels were markedly increased (Figure 6D, $P < 0.001$). Additionally, there was a significant increase in spleen weight (Figure 6E, $P < 0.001$) and a decrease in mice body weight (Figure 6F, $P < 0.001$). These observations, from various perspectives, are similar to the clinical symptoms of AIT and consistent with previous studies.[8] These findings provide support for further animal experiment validation.

Validation of AIM2, ZBP1, MLKL, NLRP6, and Fas by qRT-PCR and Immunohistochemistry

We further assayed the selected genes using qRT-PCR. Notably, compared to the control group, the mRNA levels of AIM2, ZBP1, MLKL, NLRP6, and Fas were significantly upregulated in the thyroid tissue of mice in the model group (Figure 7A, $P < 0.001$ or $P < 0.01$) Additionally, immunohistochemical analysis revealed a marked increase in the positive expression of AIM2, ZBP1, MLKL, NLRP6, and Fas proteins in the thyroid tissue of the AIT group compared to the control group (Figure 7B). These genes are identified as crucial core genes influencing the progression of AIT, consistent with our bioinformatics analysis results.

Experimental Validation and Diagnostic Evaluation of Panoptosis-Related Biomarkers in Autoimmune Thyroiditis

To validate the bioinformatically identified candidates, we performed qRT-PCR analysis using peripheral blood samples from clinically confirmed autoimmune thyroiditis (AIT) patients. The results demonstrated significant upregulation of AIM2 (3.2-fold, $P < 0.001$), ZBP1 (2.8-fold, P = 0.003), MLKL (2.3-fold, $P = 0.007$), NLRP6 (1.9-fold, $P = 0.015$), and Fas (1.6-fold, $P = 0.028$) mRNA levels in the AIT cohort compared with healthy controls (HC group) (Figure 8A). Receiver operating characteristic (ROC) analysis further revealed robust diagnostic performance, with area under the curve (AUC) values of 0.902 (95% CI: 0.854–0.943) for AIM2, 0.890 (0.833–0.938) for ZBP1, 0.788 (0.718–0.851) for MLKL, 0.733 (0.657–0.802) for NLRP6, and 0.721 (0.642–0.793) for Fas. Notably, all biomarkers exceeded the minimum discriminative threshold (AUC > 0.7) (Figure 8B), establishing their collective potential as a multi-analyte diagnostic panel for AIT.

Discussion

Autoimmune thyroiditis (AIT) is one of the most prevalent autoimmune diseases, imposing an increasing health burden on individuals and society.[3] From a pathological perspective, thyroid autoantigens serve as the driving force for autoimmune responses, with various immune cell types and associated molecules amplifying these responses, leading to uncontrollable inflammatory reactions across multiple bodily systems.[17] However, the molecular mechanisms underlying the autoimmune attack on thyroid tissue triggered by abnormal immune functions of cellular subsets remain largely unexplained. The introduction of the concept of panoptosis, a newly defined mode of inflammatory cell death, holds promise for elucidating the immune regulatory network involved in the pathogenesis of AIT and exploring a novel research direction.

Therefore, our study utilized single-cell RNA sequencing datasets from healthy individuals, tissues from patients with HT, and PBMCs to evaluate the expression distribution of PANoptosis -related genes across cellular subpopulations. The results indicated that PANoptosis -related genes were expressed in multiple cell types, with the AIM2 gene showing the most prominent expression in proliferating cells (cells with potential differentiation capacity). Subsequently, we further applied single-sample gene set enrichment analysis (ssGSEA) to assess the correlation between immune cells and inflammatory effects between the AIT group and the control group. Additionally, we integrated PANoptosis -related genes with immune functions to screen for the gene modules most significantly associated with the immune-

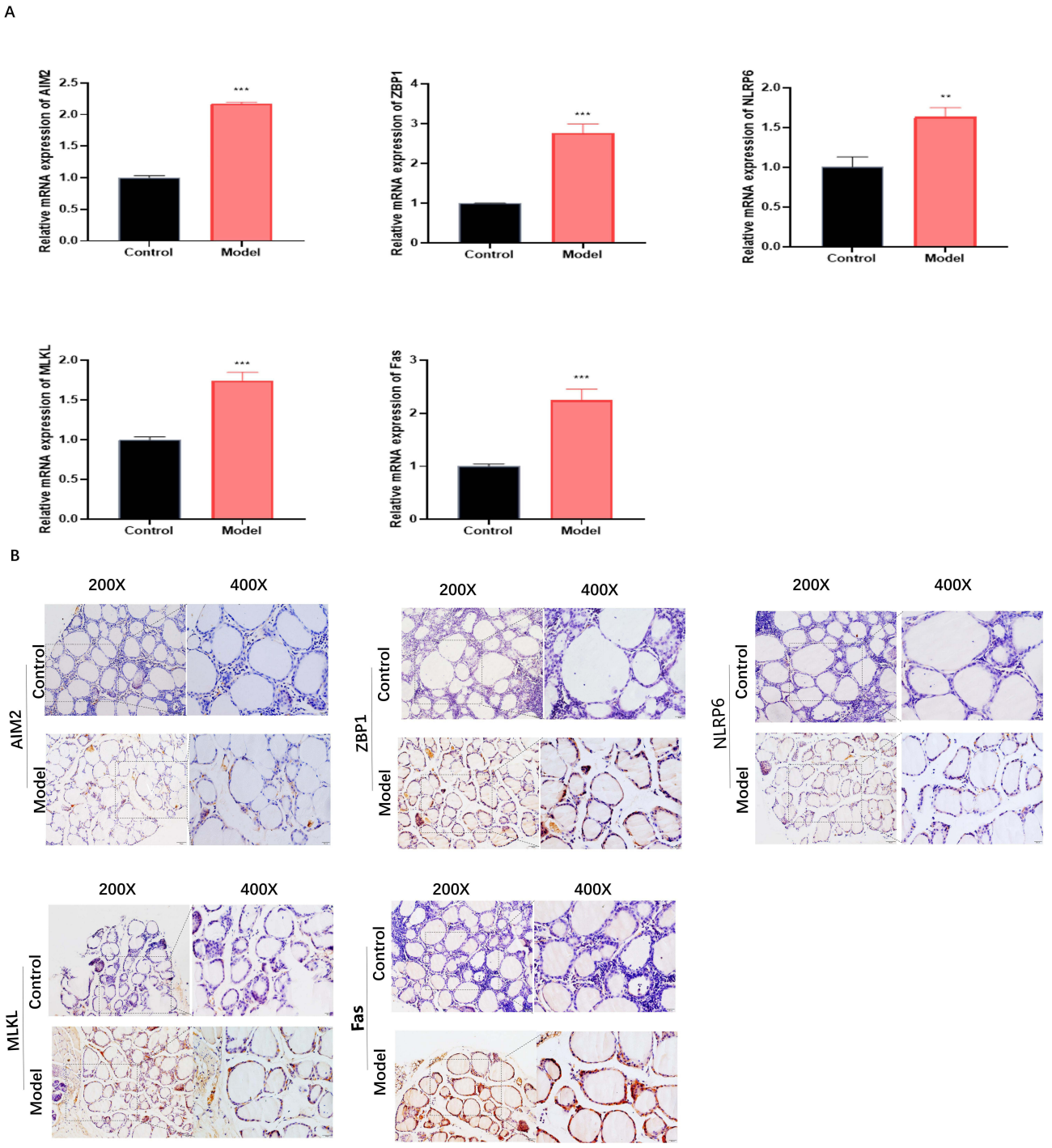

Figure 7 Validation of AIM2, ZBP1, MLKL, NLRP6, and Fas by qRT-PCR and Immunohistochemistry. (**A**) Validation of panoptosis-related genes in Module 5 using qRT-PCR, showing the relative mRNA expression levels of AIM2, ZBP1, MLKL, NLRP6, and Fas. (**B**) Immunohistochemical analysis revealing the distribution of AIM2, ZBP1, MLKL, NLRP6, and Fas in the tissue. ***$P < 0.001$, **$P < 0.01$, *$P < 0.05$ vs Control group. Magnification: 200×, 400×(n=3).
Abbreviation: qRT–PCR, quantitative reverse transcription–PCR.

inflammatory effects of AIT. Our findings revealed that the PANoptosis -related genes AIM2, ZBP1, MLKL, NLRP6, and Fas were most closely correlated with the pro-inflammatory response in AIT, with AIM2 emerging as the core HUB gene. Furthermore, we subsequently validated our findings through RT-qPCR and immunohistochemical staining using both animal and clinical samples, confirming consistency with the results obtained from bioinformatics tools. Moreover,

https://doi.org/10.2147/JIR.S525270

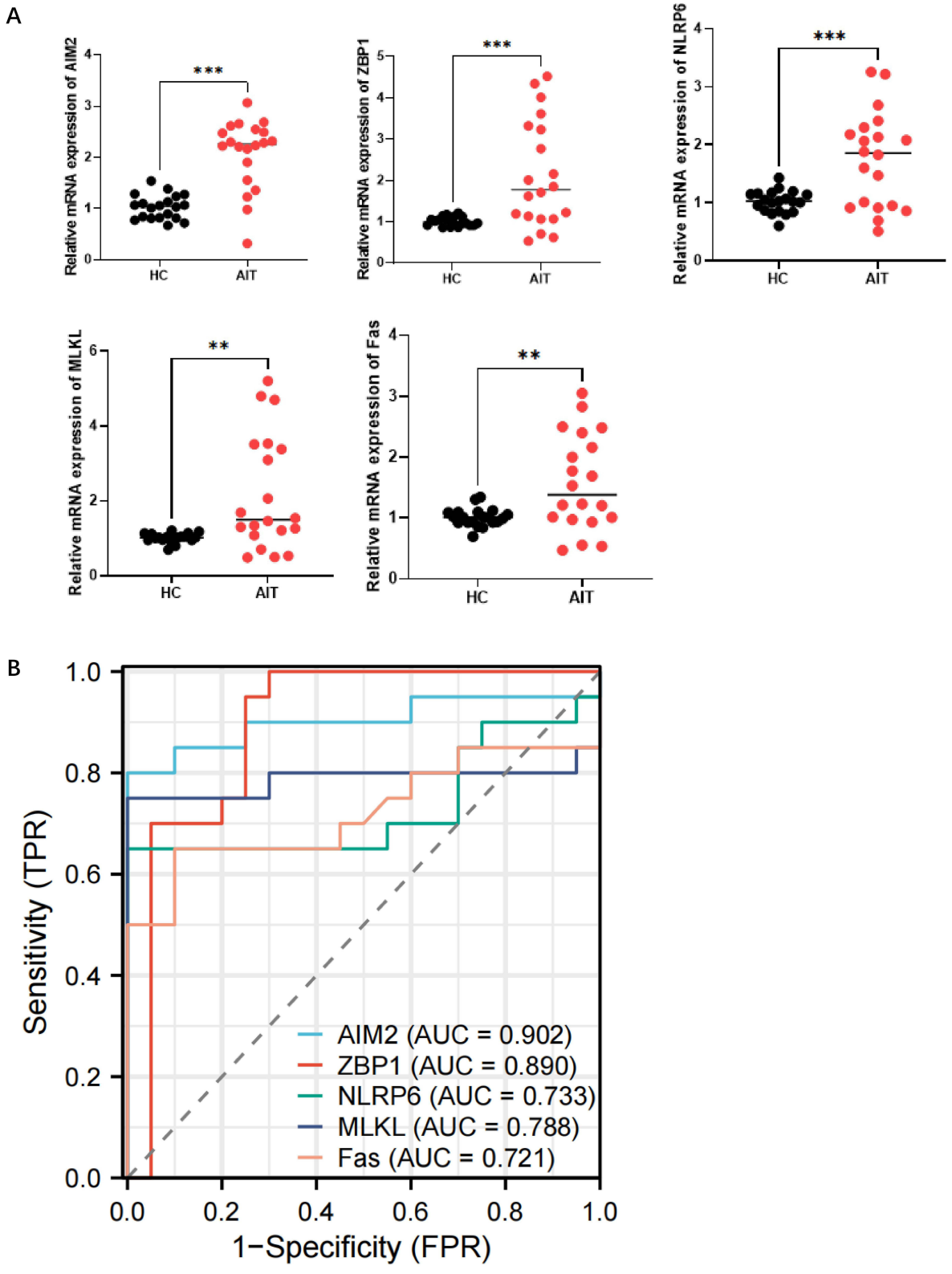

Figure 8 Experimental validation and diagnostic evaluation of panoptosis-related biomarkers in autoimmune thyroiditis. (**A**) Using qRT-PCR to validate the panoptosis-related genes in Module 5, the relative mRNA expression levels of AIM2, ZBP1, MLKL, NLRP6, and FAS in the peripheral blood of AIT patients were determined. (**B**) Diagnostic capacity assessment using ROC analysis.$^{**}P < 0.001$, $^{**}P < 0.01$, $^{*}P < 0.05$ vs HC group (n = 20).

Abbreviations: ROC, receiver operating characteristic; AUC, area under the ROC curve; HC group, healthy control (HC) group;AIT group,AIT patient group.

ROC curve analysis demonstrated that these genes exhibited strong diagnostic efficacy, reaffirming their critical roles in AIT. Collectively, our results revealed the key regulatory role of PANoptosis in AIT progression. These findings enhance our understanding of the underlying mechanisms of AIT and provide a foundation for future in-depth exploration of PANoptosis-mediated regulation in AIT and immune regulatory networks.

HT represents a classic disease type of AIT. It has been reported that the typical pathological feature of AIT is the immune infiltration of lymphocytes within the thyroid tissue, which exacerbates the inflammatory response and plays a pivotal role in the pathogenesis of AIT. However, the underlying mechanisms related to this process remain poorly understood. Excitingly, Zhang et al conducted an in-depth analysis of the cellular components in thyroid tissue and PBMCs from AIT patients using single-cell RNA sequencing technology, revealing the crucial roles of specific stromal cells and immune cells in the thyroid microenvironment in lymphocyte infiltration and thyroid cell destruction.[3] Nevertheless, the potential mechanisms underlying immune cell infiltration in the thyroid tissue of AIT patients are still unclear. Intriguingly, the recent introduction of the concept of panoptosis has provided a new perspective for the study of autoimmune diseases, including AIT. The significance of panoptosis in immune infiltration has also been demonstrated in several recent correlation studies.[18,19] PANoptosis is mediated by the assembly of a multiprotein signal complex called inflammatory bodies, which is the central hub of triggering many aspects of cell death in the form of PANoptosis and inflammatory immune response. The PANoptosome is comprised of sensors that respond to stimuli, effectors that execute functions, and an adaptor that links the sensor to the effector. The sensor, by engaging with upstream stimuli and relaying signals downstream, orchestrates the assembly of a molecular scaffold that incorporates key molecules involved in pyroptosis, apoptosis, and necroptosis.[20] Studies have indicated that the expression of PCD-related genes is positively correlated with the serum levels of thyroid peroxidase and thyroglobulin antibodies. Immune cell subsets, such as dendritic cells, can capture and present antigens from their own tissues, thereby fueling a robust immune response by T cells. These findings underscore the crucial role of immune cells in the pathogenesis of AIT.[21]

In this study, we demonstrated that the PANpoptosis gene set is widely distributed across various cell subpopulations with high abundance, among which the panoptosis-related AIM2 gene exhibits the most prominent expression in proliferating cells (Proliferating cells represent a subset of B cells. This cell population expresses not only the characteristic genes of B cells but also proliferation-associated marker genes). Panoptosis may initiate PANpoptosis by upregulating AIM2 expression, playing a crucial role in the onset and progression of immune inflammation in AIT. Furthermore, we conducted an in-depth immune infiltration analysis, categorizing the immune cell heatmaps of the two groups into three layers: anti-inflammatory, pro-inflammatory, and other immune cells. The results of the ssGSEA assessment revealed that compared to non-HT individuals, HT patients exhibit a stronger pro-inflammatory effect. The pro-inflammatory cells include central memory $CD4^+$T cells, central memory $CD8^+$T cells, effector memory $CD4^+$T cells, effector memory $CD8^+$T cells, natural killer cells, natural killer T cells, Type 1 T helper cells, and Type 17 T helper cells.

Previous studies have demonstrated that the balance between CD4+ T cells and their subsets is crucial for maintaining immune homeostasis and preventing the onset and progression of AIT. Both our previous research and studies by other scholars have shown that the imbalance of Th1 and Th17 cell subsets is a key factor in the pathogenesis of AIT.[17,] Th1 and Th17 cells mediate inflammatory damage in AIT by secreting pro-inflammatory cytokines such as IFN-γ and IL-17, and they also promote the activation of cells like macrophages, thereby exacerbating the destruction of thyroid tissue.[10,22] Sharma et al,[23] derived an iNKT cell line from NOD·$H2^{h4}$ mice, and after adoptive transfer into syngeneic recipient mice, this cell line rapidly secreted multiple cytokines, significantly enhancing AIT symptoms in the recipient mice. This was manifested by increased inflammatory cell infiltration in the thyroid tissue and elevated anti-thyroglobulin antibody levels, confirming the marked responsiveness of the iNKT cell line to TG. Furthermore, studies have shown that the number of CD8+ T cells significantly increases as the disease progresses. These cells can induce apoptosis of thyroid cells by releasing cytotoxic molecules such as perforin and granzyme, thereby exacerbating the damage to thyroid tissue. NK cells, as an important component of innate immunity, also play a significant role in the pathogenesis of HT. They can directly recognize and kill thyroid cells expressing abnormal MHC molecules and further exacerbate the destruction of thyroid tissue through ADCC.[22] This process is closely associated with the activation of Th1 cells, and the interactions among these immune cell subsets jointly promote the pathological process of AIT. Moreover, panoptosis-related genes are expressed to varying degrees in these immune cell subsets of AIT patients. Based on the findings of this study, further

investigation into their specific biological roles in AIT and the interaction mechanisms among immune subsets is crucial for elucidating the regulatory network of AIT's pathological mechanisms, identifying potential therapeutic targets, and improving the treatment of AIT.

However, it is insufficient to explain the onset of diseases solely from the perspectives of cell subtype abundance or functional modules, and the integration of both is essential. Therefore, we subsequently constructed a weighted gene co-expression network and utilized WGCNA analysis to correlate highly co-expressed gene modules with immune functions. Our findings revealed that the PANoptosis-related genes AIM2, ZBP1, MLKL, NLRP6, and Fas are key genes in the pro-inflammatory response of HT. Among these, the AIM2 gene emerges as a potential core HUB gene (kme=0.55) in the PANoptosis pathway.

AIM2, as an innate immune receptor, recognizes dsDNA in the cytoplasm and assembles into the AIM2 inflammasome. This not only mediates immune inflammatory responses but also serves as a bridge linking innate immunity and cell death. It can form the AIM2 PANoptosome complex, driving inflammatory signaling and the occurrence of panoptosis. AIM2 plays a crucial role in development, inflammatory diseases, and cancer.[14,24] Studies have shown that in mice lacking AIM2, the occurrence of panoptosis is significantly inhibited, accompanied by an increase in viral and bacterial loads and a decrease in mice survival rates. These findings highlight the potential role of AIM2 and its mediated panoptosis in autoimmune diseases. Consistent with these reports, we observed a marked upregulation of AIM2 in the thyroid tissue of mice with AIT. AIM2-mediated panoptosis may be the initiating factor for immune-inflammatory infiltration in the thyroid tissue. Clinical validation in AIT patients confirmed significant AIM2 upregulation with diagnostic efficacy.

ZBP1, also known as DNA-dependent activator of interferon regulatory factors (DAI) or DLM-1, serves as a crucial innate immune sensor that mediates panoptosis, akin to AIM2. It has the capability to recognize viral RNA products and endogenous nucleic acid ligands, and assembles into a panoptotic complex. During development, ZBP1 perceives endogenous transcripts, thereby inducing programmed cell death and inflammation.[25] In the course of disease progression, ZBP1-mediated panoptosis constitutes a key pathological mechanism underlying inflammation-related disorders. During β-coronavirus infection,IFN treatment markedly upregulates ZBP1 expression, subsequently triggering panoptosis, which is closely associated with disease severity and prognosis.[26] Furthermore, ZBP1 interacts with molecules such as RIPK3 to form the ZBP1-PANoptosome complex, leading to cell death and the release of inflammatory cytokines. In inflammatory bowel disease, ZBP1-dependent necroptosis is activated, contributing to the onset and progression of the disease.[27] Consistent with previous literature, we observed a significant upregulation of ZBP1, uncovering its potential role in mediating panoptosis in AIT.

NLRP6 is an emerging inflammasome sensor discovered in recent years, which leads to the cleavage and activation of caspase-1, promoting the release of antimicrobial molecules and the occurrence of pyroptosis. It exhibits complex roles in various disease models.[28] Studies have revealed that NLRP participates in the onset and progression of colorectal cancer by regulating PANoptosis.[29] NLRP6 deficiency results in a significant expansion of a novel $CD103^+$ B cell subset in mice, delaying and protecting NOD mice from the development of type 1 diabetes.[30] In the present study, NLRP6 was markedly elevated in the thyroid tissue of mice with AIT, suggesting that NLRP6 holds promise as a new direction for investigating the pathogenesis of AIT.

Additionally, panoptosis, as a highly coordinated and homeostatically regulated form of programmed cell death, exhibits key features of pyroptosis, apoptosis, and/or necroptosis, and cannot be characterized in isolation. These three forms of cell death intertwine and cooperate during the panoptotic process, collectively determining the ultimate fate of the cell. In our study conclusions, MLKL and Fas emerge as the key executors of necroptosis and apoptosis, respectively. Specifically, Fas is a death receptor in the extrinsic pathway, and studies have shown that FAS plays a pivotal role in the extrinsic apoptotic pathway of autoimmune diseases. The FAS gene −670A/G polymorphism is associated with a reduced risk of HT in Asians, leading to decreased expression of soluble FAS and subsequently reduced apoptosis of autoreactive lymphocytes.[31] Fas primarily binds to its ligand, recruiting and activating caspase-8, which triggers a caspase cascade, ultimately resulting in cell apoptosis.[32] When caspase-8 activity is inhibited, it promotes the formation of the necrosome, where RIPK3 phosphorylates MLKL. The activated MLKL translocates to the cell membrane and mediates changes in membrane permeability, ultimately leading to necroptosis. Furthermore, active MLKL can activate the NLRP3

inflammasome, thereby exacerbating pyroptosis.[33] There is also a certain connection between MLKL-mediated necroptosis and apoptosis. For instance, in some cell types, activation of MLKL may lead to mitochondrial damage and the release of cytochrome c.[34] Metformin significantly alleviates renal injury caused by lupus nephritis, an autoimmune disease, through the AMPK/STAT3 signaling pathway. This process involves inhibiting MLKL-mediated necroptosis and inflammation, thereby protecting renal function.[35]

Similarly, the aforementioned reports demonstrate the existence of a complex dynamic molecular network among these processes, which cannot be discussed in isolation, thereby indirectly elucidating that PANoptosis serves as a reliable effector mechanism in the immune-inflammatory cascade of AIT. Collectively, these findings indicate that AIM2, ZBP1, NLRP6, MLKL, and Fas, as key regulatory genes of PANoptosis, play central roles in modulating pro-inflammatory responses in AIT. Subsequently, we validated the significant upregulation of these genes at both transcriptional and protein levels using clinical and animal samples, demonstrating robust diagnostic efficacy. These results align with bioinformatics insights derived from single-cell sequencing, thereby enhancing the credibility of our study. This further supports that these five genes serve as potential biomarkers for AIT, and AIM2 acts as a critical mechanistic driver of immune inflammation in AIT. Collectively, these discoveries establish a scientific foundation for elucidating immune dysregulation in AIT, refining the PANoptosis-mediated pathological regulatory network, and exploring therapeutic targets for this disease. More importantly, Guo et al's (2018) study revealed that programmed cell death mediated by genes such as AIM2 occurs in thyroid follicular epithelial cells (TFCs) of patients with autoimmune thyroiditis (AIT). The release of damage-associated molecular patterns (DAMPs) from these dying cells can further activate the immune system, forming a positive feedback loop involved in the pathogenesis and progression of AIT. This suggests that AIM2-mediated pan-apoptosis may be a critical pathogenic mechanism in AIT. In vitro experiments simulating the pathogenic environment of AIT further confirmed the activation of inflammasomes and programmed cell death in TFCs, which subsequently modulate immune and inflammatory responses, driving the occurrence and development of AIT.

However, there are still some limitations of the study that need to be emphasized. Firstly, the data source was obtained from public databases, and input errors could not be assessed. Although preclinical and clinical validations have been conducted, further investigations across diverse AIT subtypes are required to confirm the generalizability of these findings. Furthermore, the pathological mechanisms and therapeutic value of PANoptosis in AIT have not yet been systematically studied in a reliable manner. Therefore, it is necessary to further elucidate the pathways and genetic mechanisms of PANoptosis in the disease progression and treatment of AIT.

Conclusion

In conclusion, our study elucidates the relationship between PANoptosis and the distribution of immune cell subsets, as well as immune-inflammatory responses in AIT, identifying five PANoptosis-related genes (AIM2, ZBP1, NLRP6, MLKL, and Fas) as novel molecular biomarkers for AIT, which exhibit favorable diagnostic performance and may serve as key regulatory mechanisms driving the immune-inflammatory response in AIT. These insights provide a novel mechanistic explanation for future research on the immune microenvironment of AIT. In the future, we will further elucidate the specific mechanisms of PANoptosis-related genes, as well as their expression regulation and interactions in different cell types, to comprehensively unveil their detailed roles in the pathogenesis of AIT. Additionally, the gene biomarkers identified in this study can serve as key molecular targets for future research. By modulating the expression or function of these genes, we anticipate advancing the development of precise immune modulation strategies for AIT and laying a theoretical foundation for establishing diagnostic and prognostic evaluation systems.

Institutional Review Board Statement

The study was conducted in accordance with the Declaration of Helsinki, and the protocol was approved by the Ethics Committee of Liaoning University of Traditional Chinese Medicine (Ethical No.: 21000042021128). All procedures adhered to the ethical standards outlined in the Guide for the Care and Use of Laboratory Animals and its subsequent amendments.

Acknowledgments

We sincerely acknowledge the official NGDC website [NGDC–GSA for Human (cncb.ac.cn)] for providing their platforms and the contributors for uploading their meaningful datasets.

Author Contributions

All authors made a significant contribution to the work reported, whether that is in the conception, study design, execution, acquisition of data, analysis and interpretation, or in all these areas; took part in drafting, revising or critically reviewing the article; gave final approval of the version to be published; have agreed on the journal to which the article has been submitted; and agree to be accountable for all aspects of the work.

Funding

This research has been supported by the National Natural Science Foundation of China (No. 82274455), the National Natural Science Foundation of China Youth Foundation Project (No: 82104805), the Shenyang Young and Middle-aged Scientific and technological Innovation talents support Program (No.: RC200370),Reserved Project for Basic Scientific Research in Higher Education Institutions - Outstanding Graduate Student Project of the Liaoning Provincial Department of Education, China (2024-JYTCB-045),2023 Basic Scientific Research Project of Liaoning Provincial Department of Education (Project No. JYTMS20231828);General Program of Joint Foundation of Liaoning Provincial Natural Science Foundation (Grant No. 2023-MSLH-147), Joint Technical Research Program of Liaoning Provincial Science and Technology Plan (Project No. 2024JH2/102600171).

Disclosure

The authors report no conflicts of interest in this work.

References

1. Tywanek E, Michalak A, Świrska J, Autoimmunity ZA. New potential biomarkers and the thyroid gland-the perspective of Hashimoto's thyroiditis and its treatment. *Int J Mol Sci*. 2024;25(9). doi:10.3390/ijms25094703
2. Hu X, Chen Y, Shen Y, et al. Global prevalence and epidemiological trends of Hashimoto's thyroiditis in adults: A systematic review and meta-analysis. *Front Public Health*. 2022;10:10:1020709. doi:10.3389/fpubh.2022.1020709
3. Zhang QY, Ye XP, Zhou Z, et al. Lymphocyte infiltration and thyrocyte destruction are driven by stromal and immune cell components in Hashimoto's thyroiditis. *Nat Commun*. 2022;13(1):775. doi:10.1038/s41467-022-28120-2
4. Guo Q, Wu Y, Hou Y. Cytokine Secretion and Pyroptosis of Thyroid Follicular Cells Mediated by Enhanced NLRP3, NLRP1, NLRC4, and AIM2 Inflammasomes Are Associated With Autoimmune Thyroiditis. *Front Immunol*. 2018;9:1197. doi:10.3389/fimmu.2018.01197
5. Malireddi RKS, Kesavardhana S, Kanneganti TD. ZBP1 and TAK1: master regulators of NLRP3 inflammasome/pyroptosis, apoptosis, and necroptosis (PAN-optosis). *Front Cell Infect Microbiol*. 2019;9:406. doi:10.3389/fcimb.2019.00406
6. Gao L, Shay C, Teng Y. Cell death shapes cancer immunity: spotlighting PANoptosis. *J Exp Clin Cancer Res*. 2024;43(1):168. doi:10.1186/s13046-024-03089-6
7. Chang X, Wang B, Zhao Y, Deng B, Liu P, Wang Y. The role of IFI16 in regulating PANoptosis and implication in heart diseases. *Cell Death Discov*. 2024;10(1):204. doi:10.1038/s41420-024-01978-5
8. Liu K, Wang M, Li D, et al. PANoptosis in autoimmune diseases interplay between apoptosis, necrosis, and pyroptosis. *Front Immunol*. 2024;15:1502855. doi:10.3389/fimmu.2024.1502855
9. Malireddi RKS, Tweedell RE, Kanneganti TD. PANoptosis components, regulation, and implications. *Aging*. 2020;12(12):11163–11164. doi:10.18632/aging.103528
10. Zhao Z, Liu Z, Song N, et al. Based on SIRT1/NF-κB/NLRP3 signal pathway to explore the effect of Yiqi Huatan Huoxue recipe on inflammatory injury in AIT mice by pyroptosis. *Comb Chem High Throughput Screen*. 2024. doi:10.2174/0113862073294048240801113424
11. Mo K, Chu Y, Liu Y, et al. Targeting hnRNPC suppresses thyroid follicular epithelial cell apoptosis and necroptosis through m(6)A-modified ATF4 in autoimmune thyroid disease. *Pharmacol Res*. 2023;196:106933. doi:10.1016/j.phrs.2023.106933
12. Grün D, van Oudenaarden A. Design and analysis of single-cell sequencing experiments. *Cell*. 2015;163(4):799–810. doi:10.1016/j.cell.2015.10.039
13. Han X, Zhou Z, Fei L, et al. Construction of a human cell landscape at single-cell level. *Nature*. 2020;581(7808):303–309. doi:10.1038/s41586-020-2157-4
14. Lee S, Karki R, Wang Y, Nguyen LN, Kalathur RC, Kanneganti TD. AIM2 forms a complex with pyrin and ZBP1 to drive PANoptosis and host defence. *Nature*. 2021;597(7876):415–419. doi:10.1038/s41586-021-03875-8
15. Newman AM, Liu CL, Green MR, et al. Robust enumeration of cell subsets from tissue expression profiles. *Nat Methods*. 2015;12(5):453–457. doi:10.1038/nmeth.3337
16. Langfelder P, Horvath S. WGCNA: an R package for weighted correlation network analysis. *BMC Bioinformatics*. 2008;9:559. doi:10.1186/1471-2105-9-559

17. Zheng H, Xu J, Chu Y, et al. A global regulatory network for dysregulated gene expression and abnormal metabolic signaling in immune cells in the microenvironment of Graves' disease and Hashimoto's thyroiditis. *Front Immunol*. 2022;13:879824. doi:10.3389/fimmu.2022.879824
18. Li J, Zhang X, Ren P, et al. Landscape of RNA-binding proteins in diagnostic utility, immune cell infiltration and PANoptosis features of heart failure. *Front Genet*. 2022;13:1004163. doi:10.3389/fgene.2022.1004163
19. Qiang S, Fu F, Wang J, Dong C. Definition of immune molecular subtypes with distinct immune microenvironment, recurrence, and PANoptosis features to aid clinical therapeutic decision-making. *Front Genet*. 2022;13:1007108. doi:10.3389/fgene.2022.1007108
20. Pandian N, Kanneganti TD. PANoptosis: a unique innate immune inflammatory cell death modality. *J Immunol*. 2022;209(9):1625–1633. doi:10.4049/jimmunol.2200508
21. Yang D, Wang X, Sun Y, Shao Y, Shi X. Identification and experimental validation of genes associated with programmed cell death in dendritic cells of the thyroid tissue in Hashimoto's thyroiditis. *Int Immunopharmacol*. 2024;142(Pt A):113083. doi:10.1016/j.intimp.2024.113083
22. Wrońska K, Hałasa M, Szczuko M. The role of the immune system in the course of Hashimoto's thyroiditis: the current state of knowledge. *Int J Mol Sci*. 2024;25(13):6883. doi:10.3390/ijms25136883
23. Sharma RB, Fan X, Caturegli P, Rose NR, Burek CL. Invariant NKT cell lines derived from the NOD·H2 mouse enhance autoimmune thyroiditis. *J Thyroid Res*. 2011;2011:895923. doi:10.4061/2011/895923
24. Oh S, Lee J, Oh J, et al. Integrated NLRP3, AIM2, NLRC4, Pyrin inflammasome activation and assembly drive PANoptosis. *Cell Mol Immunol*. 2023;20(12):1513–1526. doi:10.1038/s41423-023-01107-9
25. Zheng M, Kanneganti TD. The regulation of the ZBP1-NLRP3 inflammasome and its implications in pyroptosis, apoptosis, and necroptosis (PANoptosis). *Immunol Rev*. 2020;297(1):26–38. doi:10.1111/imr.12909
26. Karki R, Lee S, Mall R, et al. ZBP1-dependent inflammatory cell death, PANoptosis, and cytokine storm disrupt IFN therapeutic efficacy during coronavirus infection. *Sci Immunol*. 2022;7(74):eabo6294. doi:10.1126/sciimmunol.abo6294
27. Wang R, Li H, Wu J, et al. Gut stem cell necroptosis by genome instability triggers bowel inflammation. *Nature*. 2020;580(7803):386–390. doi:10.1038/s41586-020-2127-x
28. Pandey A, Li Z, Gautam M, Ghosh A, Man SM. Molecular mechanisms of emerging inflammasome complexes and their activation and signaling in inflammation and pyroptosis. *Immunol Rev*. 2025;329(1):e13406. doi:10.1111/imr.13406
29. Sharma BR, Kanneganti TD. Inflammasome signaling in colorectal cancer. *Transl Res*. 2023;252:45–52. doi:10.1016/j.trsl.2022.09.002
30. Pearson JA, Peng J, Huang J, et al. NLRP6 deficiency expands a novel CD103(+) B cell population that confers immune tolerance in NOD mice. *Front Immunol*. 2023;14:1147925. doi:10.3389/fimmu.2023.1147925
31. Yan H, Hong Y, Cai Y. Association between FAS gene −670 A/G and −1377 G/A polymorphisms and the risk of autoimmune diseases: a meta-analysis. *Biosci Rep*. 2020;40(1). doi:10.1042/bsr20191197
32. Pasparakis M, Vandenabeele P. Necroptosis and its role in inflammation. *Nature*. 2015;517(7534):311–320. doi:10.1038/nature14191
33. Conos SA, Chen KW, De Nardo D, et al. Active MLKL triggers the NLRP3 inflammasome in a cell-intrinsic manner. *Proc Natl Acad Sci U S A*. 2017;114(6):E961–e969. doi:10.1073/pnas.1613305114
34. Wang X, Jiang W, Yan Y, et al. RNA viruses promote activation of the NLRP3 inflammasome through a RIP1-RIP3-DRP1 signaling pathway. *Nat Immunol*. 2014;15(12):1126–1133. doi:10.1038/ni.3015
35. Chen XC, Wu D, Wu HL, et al. Metformin improves renal injury of MRL/lpr lupus-prone mice via the AMPK/STAT3 pathway. *Lupus Sci Med*. 2022;9(1):e000611. doi:10.1136/lupus-2021-000611